Draft version November 4, 2008
Preprint typeset using LaTeX style emulateapj v. 03/07/07

CURVATURE EFFECT OF A NON-POWER-LAW SPECTRUM AND SPECTRAL EVOLUTION OF GRB X-RAY TAILS

Bin-Bin Zhang[1], Bing Zhang [1], En-Wei Liang [2], Xiang-Yu Wang [3]

Draft version November 4, 2008

ABSTRACT

The apparent spectral evolution observed in the steep decay phase of many GRB early afterglows raises a great concern of the high-latitude "curvature effect" interpretation of this phase. However, previous curvature effect models only invoked a simple power law spectrum upon the cessation of the prompt internal emission. We investigate a model that invokes the "curvature effect" of a more general non-power-law spectrum and test this model with the Swift/XRT data of some GRBs. We show that one can reproduce both the observed lightcurve and the apparent spectral evolution of several GRBs using a model invoking a power-law spectrum with an exponential cut off. GRB 050814 is presented as an example.

Subject headings: gamma-rays: bursts

1. INTRODUCTION

Most of the early X-Ray afterglows detected by Swift (Gehrels et al. 2004) show a steep decay phase around 100∼1000 seconds after the burst trigger (Tagliaferri et al. 2005). The main characteristics of this steep decay phase include the following. (1) It connects smoothly to the prompt γ-ray light curve extrapolated to the X-ray band, suggesting that it is the "tail" of the prompt emission (Barthelmy et al. 2005, O'Brien et 2006, Liang et al 2006). (2) The decay slope is typically $3 \sim 5$ when choosing the GRB trigger time as the zero time point t_0 (Tagliaferri et al. 2005; Nousek et al. 2006; Zhang et al 2006). (3) The time-averaged spectral index of the steep decay phase is much different from that of the later shallow decay phase, indicating that it is a distinct new component that is unrelated to the conventional afterglow components (Zhang et al 2006; Liang et al. 2007). (4) Strong spectral evolution exists in about one third of the bursts that have a steep decay phase (Zhang et al. 2007, hereafter ZLZ07; Butler & Kocevski 2007; Starling et al. 2008). All these features suggest that the steep decay phase holds the key to understand the connection between the prompt emission (internal) phase and the traditional afterglow (external) phase. Any proposed model (see Mészáros 2006; Zhang 2007 for reviews) should be able to explain these features.

The so called "curvature effect", which accounts for the delayed photon emission from high latitudes with respect to the line of sight upon the abrupt cessation of emission in the prompt emission region (Fenimore et al. 1996; Kumar & Panaitescu 2000; Dermer 2004; Dyks et al. 2005; Qin 2008a), has been suggested to play an important role in shaping the sharp flux decline in GRB tails (Zhang et al. 2006; Liang et al. 2006; Wu et al. 2006; Yamazaki et al. 2006). In the simplest model, it is assumed that the instantaneous spectrum at the end of the prompt emission is a simple power law with a spectral index β. The predicted temporal decay index of the emission is (with the convention $F_\nu \propto t^{-\alpha}\nu^{-\beta}$)

$$\alpha = 2 + \beta \ , \tag{1}$$

if the time origin to define the $\log - \log$ light curve, t_0, is taken as the beginning of the last emission episode before the cessation of emission. Adopting a time-averaged β in the tails, Liang et al. (2006) found that Eq.(1) is generally valid. The strong spectral evolution identified in a group of GRB tails (ZLZ07) apparently violates Eq.(1), which is valid only for a constant β. ZLZ07 then investigated a curvature effect model by assuming a structured jet with varying β at different latitudes and that the line of sight is near the jet axis[4]. One would then expect that Eq.(1) is roughly satisfied, with both α and β being time-dependent. ZLZ07 found that this model does not fit the data well.

These facts do not rule out the curvature effect interpretation of GRB tails, however. This is because the instantaneous spectrum upon the cessation of prompt emission may not be a simple power law. If the spectrum has a curvature, as the emission from progressively higher latitudes reach the observer, the XRT band is sampling different segments of the intrinsic curved spectrum (Fig.1). This would introduce an apparent spectral evolution in the decaying tail. The main goal of this paper is to test this more general curvature effect model using the available Swift XRT data.

2. CURVATURE EFFECT OF A NON-POWERLAW SPECTRUM

We consider a general non-power-law spectrum in the form of

$$F_\nu(\nu) = F_{\nu,c} G(\nu) \ , \tag{2}$$

where $G(\nu)$ is the function form of the spectrum with a characteristic frequency ν_c so that $G(\nu_c)$=1, and $F_{\nu,c} = F_\nu(\nu_c)$ is the normalization of the spectrum at $\nu = \nu_c$.

The curvature effect states that given a same spectrum at different latitudes with respect to the line of sight,

[1] Department of Physics and Astronomy, University of Nevada, Las Vegas, NV 89154, USA; zbb,bzhang@physics.unlv.edu
[2] Department of Physics, Guangxi University, Nanning 530004, China
[3] Department of Astronomy, Nanjing University, Nanjing 210093, China

[4] Notice that this structured jet model is different from the traditional one that invokes an angle-dependent energy/Lorentz factor, but not the spectral index (Zhang & Mészáros 2002; Rossi et al. 2002).

TABLE 1
BEST-FITTING PARAMETERS AND THEIR 1-SIGMA ERRORS FOR THE CUTOFF POWER CURVATURE EFFECT MODEL FOR GRB050814.

$N_{0,p}$	$E_{c,p}$(keV)	Γ	t_0(s)	nH_{host}	k	χ^2/dof
0.67(0.12)	10.2(1.3)	1.56(0.25)	103.5(3.4)	0.002(0.04)	1 (fixed)	10.7/9

one has $F_{\nu,c} \propto \mathcal{D}^2$ and $\nu_c \propto \mathcal{D}$, where $\mathcal{D}$ is the Doppler factor. If the high-latitude angle $\theta \gg \Gamma$, the Dopper factor $\mathcal{D} \propto t^{-1}$, so that $F_{\nu,c} \propto t^{-2}$, $\nu_c \propto t^{-1}$ (Kumar & Panaitescu 2000). Considering the t_0 effect (Zhang et al. 2006; Liang et al. 2006), this can be written as

$$F_{\nu,c}(t) = F_{\nu,c,p}\left(\frac{t-t_0}{t_p-t_0}\right)^{-2} \quad (3)$$

and

$$\nu_c(t) = \nu_{c,p}\left(\frac{t-t_0}{t_p-t_0}\right)^{-1} \quad (4)$$

for $t \gg t_p$, where t_0 refers to the time origin of the last pulse in the prompt emission and t_p is the epoch when the curvature-effect decay starts (or the "peak" time of the lightcurve), $F_{\nu,c,p} = F_{\nu,c}(t_p)$ and $\nu_{c,p} = \nu_c(t_p)$. Notice that in the case of $G(\nu) = (\nu/\nu_c)^{-\beta}$ (a pure power law spectrum), one derives $F_\nu \propto (t-t_0)^{-\beta-2}$. This is the relation Eq.(1).

We consider several physically motivated non-powerlaw spectra with a characteristic frequency ν_c, including the cut-off power law spectrum and the Band-function (Band et al. 1993). To explore the compatibility with the data, we also investigate different forms of the cutoffs with varying sharpness. In all cases, the $F_{\nu_p}(t)$ and $\nu_p(t)$ follow Eqs.(3) and (4). When $\nu_c(t)$ drops across an observational narrow energy band, e.g. the Swift/XRT band, it introduces an apparent spectral softening with time, which, if fitted by a power law, shows an increase of photon index with time. In the meantime, the flux within the observing band drops down rapidly, leading to an apparent steep decay phase in the lightcurve (Fig.1).

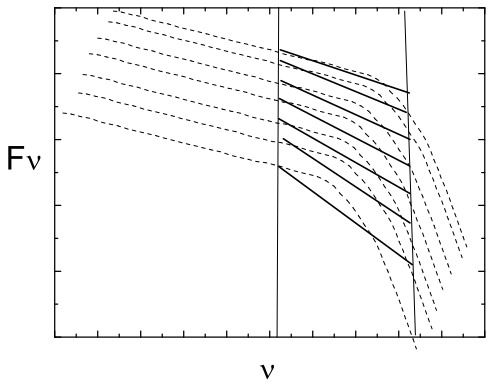

FIG. 1.— A schematic picture showing that shifting a set of non-power-law spectra in time can equivalently give an apparent spectral evolution in a fixed band. The dashed lines represent a set of exponential-like spectra, whose $F_{\nu_p}(t)$ and $\nu_p(t)$ drop down with time according to Eqs. (3) and (4). The two vertical solid lines bracket the observed energy band. The thick solid lines denote the effective power law fits to the time-dependent spectra at each time step.

3. DATA REDUCTION AND SIMULATION METHOD

We consider a time-dependent cutoff power law photon spectrum taking the form of

$$N(E,t) = N_0(t)\left(\frac{E}{1\ \mathrm{keV}}\right)^{-\Gamma}\exp\left[-\left(\frac{E}{E_c(t)}\right)^k\right] \quad (5)$$

where $\Gamma = \beta + 1$ is the power law photon index, and k is a parameter to define the sharpness of the high energy cutoff in the spectrum, $E_c(t)$ is the time-dependent characteristic photon energy, and $N_0(t)$ is a time-dependent photon flux (in units of photons $\cdot$ keV^{-1}cm^{-2}s^{-1}) at 1 keV (Arnaud 1996). The choice of this function was encouraged by the fact that the spectral evolution of some GRB tails can be fitted by such an empirical model (Campana et al. 2006; ZLZ07; Yonetoku et al. 2008). According to Eqs.(3) and (4), and noticing the conversion between the photon flux and the emission flux density, i.e. $F_\nu \propto EN(E)$, we get

$$E_c(t) = E_{c,p}\left(\frac{t-t_0}{t_p-t_0}\right)^{-1} \quad (6)$$

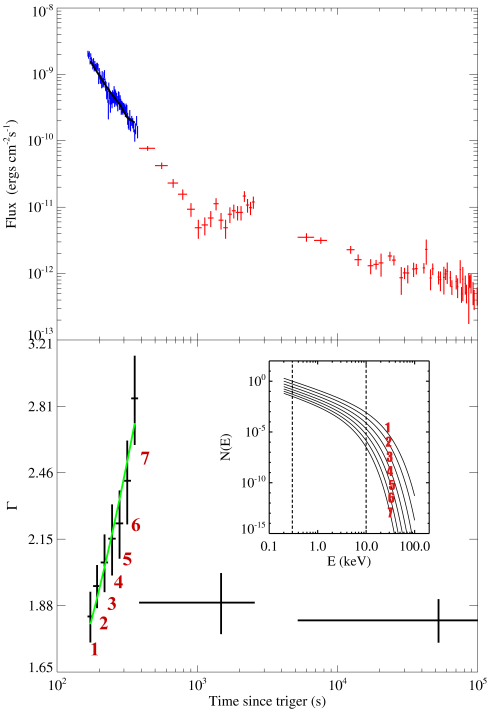

FIG. 2.— The lightcurve (upper panel) and spectral evolution (lower panel) of the X-ray tail of GRB 050814 with the best-fit theoretical model (black curve in upper panel and green curve in lower panel). The blue and red data points are the window timing and photon counting data, respectively. The inset shows time-dependent theoretical spectra with the XRT band (0.3-10 keV) bracketed by two vertical lines. The integers denote the time segments for the time-resolved spectral analysis.

and $N(E_c,t) = N_{c,p}\left[(t-t_0)/(t_p-t_0)\right]^{-1}$, where $N_{c,p} = N(E_c,t_p)$, and $E_{c,p} = E_c(t_p)$. This gives

$$N_0(t) = N_{0,p}\left(\frac{t-t_0}{t_p-t_0}\right)^{-(1+\Gamma)}. \quad (7)$$

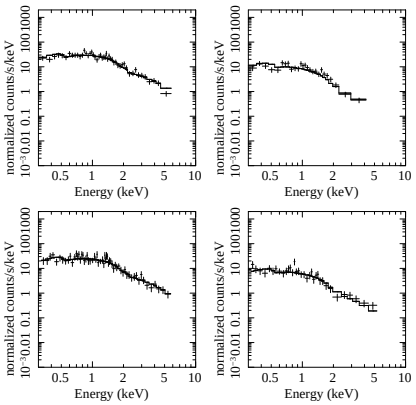

FIG. 3.— *Upper panel*: Examples of simulated time-dependent spectra of GRB050814 with the best-fit parameters. The time intervals are 1,6 repectively as denoted in Fig. 2. In each panel, the data histogram displays the simulated spectrum, and the solid line displays the best-fit ($\chi^2/dof = 39.0/61, 25.2/25$) power law model ($wabs * zwasb * powerlaw$ in XSPEC) that is used to derive the time-dependent photon index Γ. *Lower pabel*: The corresponding observed spectrum in the three time intervals and their power law fits ($\chi^2/dof = 47.1/46, 22.0/19$).

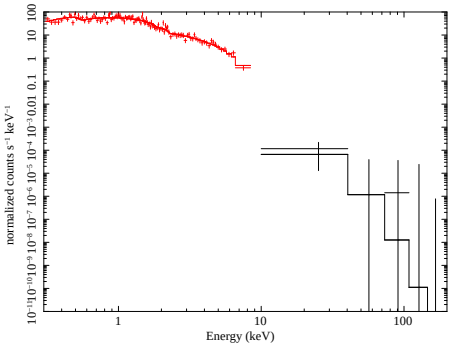

FIG. 4.— The simulated cut-off power law spectrum at $t_p = 144$ s based on the best fit model confronted by the BAT data in the time interval $(141.5 - 146.5)$ s. The reduced χ^2 of the fitting is 1.2 with dof= 197.

Notice that t_p is the beginning of the steep decay, which is a parameter that can be directly constrained by the data. For a complete lightcurve, we read t_p off from the lightcurve. In the case of an observational gap, usually t_p can be reasonably fixed to the end of the prompt emission. We therefore do not include this parameter into the fits, and derive the other five parameters, namely, $N_{0,p}$, $E_{c,p}$, Γ, t_0, and k from the data. At any time t, the model spectrum can be determined once these parameters are given. One can then confront the model with the real GRB data.

The procedure includes the following steps. (1) For a given burst, we extract its Swift/XRT light curve and n slices of time-dependent spectra using the standard HEASoft/Swift Package. The details of the data reduction method were described in ZLZ07. (2) Given a trial set of parameters in the theoretical spectra[5] $\{N_{0,p}$, $E_{c,p}$, Γ, $t_0\}$, using Eqs.(5-6) we model n time-dependent *theoretical spectra* that correspond to the time bins that are used to derive the time-dependent observed spectra. (3) Based on the theoretical spectra of each time slice, we simulate the corresponding *model spectra* by taking account of the observational effects, including the Swift/XRT response matrix, the absorption column densities (N_H) of both the Milky Way (extracted from the observations from step 1) and the host galaxy of the burst (a free parameter), the redshift (if applicable), and a Poisson noise background. Notice that $n_{H,host}$ is another parameter introduced in the model spectra (besides the other parameters introduced in the theoretical spectra). All these faked spectra can be obtained using HEASoft (Version 6.4) and Xspec (Version 12.4) (4) We fit the faked model spectra with a simple power law model, i.e. $wabs * wabs * powerlaw$ (or $wabs * zwabs * powerlaw$ if the redsift is available) in XSPEC and get the simulated fluxes and spectral indices of the n slices. Here the column densities of both the Milk Way and the host galaxy are fixed to the obsered values as in Step 1. (5) We compare the simulated fluxes and spectral indices with the observed ones and access the goodness of the fits using χ^2 statistics. (6) We refine the trial set of parameters based on the comparison and repeat steps (2)-(5) when necessary. We test whether we can reach a set of best-fitting parameters that can reproduce both the light curve and the apparent spectral evolution as observed.

4. AN EXAMPLE: GRB050814

We apply the method to GRB050814, a typical burst with well-observed X-ray tail with strong spectral evolution. As seen in Fig.2, the tail has a steep decay index of ~ 3.2, and a strong spectral evolution is apparent at[6] $t < 600$ s. These features are common in most of the GRB X-ray tails. We first fix $k = 1$ in Eq. 5, which corresponds to the simplest cutoff powerlaw model. The initial trial parameters we choose are (Γ, $N_{0,p}$, t_0, $E_{p,0}$, $n_{H,host}$) $= (1.2, 0.4, 72.0, 30.0, 0.05)$. The peak time t_p is fixed to 143.6 s, which corresponds to the end of the prompt emission. Some IDL scripts are developed to follow the procedure described in §3 to automatically search for the best-fit parameters to match both the observed light curve and the time-dependent spectral index. The final best-fitting parameters are shown in Table 1. The corresponding simulated light curve (black curve) and spectral indices (green curve) are shown in Fig.2. Figure 2 suggests that the sharp decay and the spectral evolution in the tail of GRB 050814 can be indeed explained by the curvature effect with a cutoff power law spectrum. In Fig.3 we present the comparison between the simualted and observed spectra in the time steps 1 and 6 (as examples), which show reasonable consistency.

Our model predicts that the prompt emission spectrum at $t_p \sim 144$ s should be a cut-off power law with the parameters in Table 1. In order to confirm this, we subtract the BAT-band spectrum in the time interval $(141.5 - 146.5)$ s, and compare with the data with the model prediction. As shown in Fig.4, the BAT data is roughly consistent with the model prediction, suggesting the validity of the model.

Some physical parameters can be constrained according to our model. The time interval from t_p to the begin-

[5] Notice that k is fixed to a certain value for a particular model, and is varied when different models are explored.

[6] The PC mode spectra become harder at the end of this tail, which might be due to the contamination of the harder shallow decay component. For simplification, we focus on the WT mode data only.

ning of the steep decay phase $t_{tail,0}$ may be related to the angular spreading time scale $\tau_{ang} = (t_{tail,0} - t_p)/(1+z)$. Noticing $z \sim 5.3$ for GRB050814 (Jakobsson et al. 2005), we can estimate the Lorentz factor of the fireball as $\Gamma = (R/2c\tau_{ang})^{1/2} \simeq 69 R_{15}^{1/2}$, where $R_{15} = R/(10^{15}$ cm) is the normalized emission radius. Since we know the spectral peak energy E_p at t_p, we can also estimate the corresponding electrons' Lorentz factor for synchrotron emission by $\gamma_{e,p} = \left[E_p/(\hbar\Gamma\frac{eB}{mc})\right]^{1/2} \sim 2.4\times10^3 R_{15}^{-1/4} B_3^{-1/2}$. From the rest frame duration of the X-ray tail we are analyzing $\tau_{tail} = (t_{tail,e} - t_{tail,0})/(1+z) \sim (378-165)/6.3 = 33.8$ s, one can constrain the minimum jet opening angle as $\theta_j > (2c\tau_{tail}/R)^{1/2} = 2.6^{\rm o} \times R_{15}^{-1/2}$. These values are generally consistent with those derived from various other methods.

We find that the abruptness parameter k cannot be very different from unity. A Band-function spectrum introduces a less significant spectral evolution and it cannot reproduce the data (cf. Qin 2008b).

5. DISCUSSIONS AND CONCLUSIONS

We have successfully modeled the lightcurve and spectral evolution of the X-ray tail of GRB050814 using the curvature effect model of a cutoff power law spectrum with an exponential cutoff ($k = 1$). It has been discussed in the literature (e.g. Fan & Wei 2005; Barniol-Duran & Kumar 2008) that the GRB central engine may not die abruptly, and that the observed X-ray tails may reflect the dying history of the central engine. If this is indeed the case, the strong spectral evolution in the X-ray tails would demand a time-dependent particle acceleration mechanism that gives a progressively soft particle spectrum. Such a behavior has not been predicted by particle acceleration theories. Our results suggest that at least for some tails, the spectral evolution is simply a consequence of the curvature effect: the observer views emission from the progressively higher latitudes from the line of sight, so that the XRT band is sampling the different segments of a curved spectrum. This is a simpler interpretation.

The phenomenology of the X-ray tails are different from case to case (ZLZ07). We have applied our model to some other clean X-Ray tails, such as GRB050724, GRB080523, and find that they can be also interpreted by this model. Some other tails have superposed X-ray flares, making a robust test of the model difficult. A systematic survey of all the data sample is needed to address what fraction of the bursts can be interpreted in this way or they demand other physically distinct models (e.g. Barniol-Duran & Kumar 2008; Dado et al. 2008). This is beyond the scope of this Letter.

We thank Pawan Kumar for stimulative discussions and comments. This work is supported by NASA NNG05GB67G, NNX07AJ64G, NNX08AN24G and NNX8AE57A (BBZ&BZ), by the National Natural Science Foundation of China under Grant 10463001 (EWL) and 10221001 (XYW), and by the National "973" Program of China under Grant 2009CB824800 (EWL& XYW). BBZ & BZ also acknowledges the President's Infrastructure Award from UNLV.

REFERENCES

Arnaud, K.A., 1996, Astronomical Data Analysis Software and Systems V, eds. Jacoby G. and Barnes J., p17, ASP Conf. Series volume 101.
Barniol Duran, R & P. Kumar, 2008, arXiv:0806.1226
Band, D et al. 1993, ApJ, 413, 281
Barthelmy, S et al. 2005, Nature, 438, 994
Butler, N. R. & Kocevki, D. 2007, ApJ, 668, 400
Campana, S. et al. 2006, Nature, 442, 1008
Dado, S., Dar, A., De Rujula, A. 2008, ApJ, 681, 1408
Dermer, C. D. 2004, ApJ, 614, 284
Dyks, J., Zhang, B. & Fan, Y. Z. 2005 , astro-ph/0511699
Fan, Y. Z. & Wei, D. M. 2005, MNRAS, 364, L42
Fenimore, E. E., Madras, C. D., & Nayakshin, S. 1996, ApJ, 473, 998
Gehrels, N., et al. 2004, ApJ, 611, 1005
Jakobsson, P. et al. 2005, A&A, 447, 897
Kumar, P. & Panaitescu, A. 2000, ApJ, 541, L51
Liang, E. W., Zhang, B., O'Brien, P. T., Willingale, R., et al. 2006, ApJ, 646, 351
Liang, E.-W., Zhang, B.-B., Zhang, B., 2007. ApJ 670, 565.
Mészáros, P. 2006, Rep. Prog. Phys. 69, 2259
Nousek, J. A., Kouveliotou, C., Grupe, D., Page, K. L., et al. 2006, ApJ, 642, 389
O'Brien, P. T., Willingale, R., Osborne, J., Goad, M. R., et al. 2006, ApJ, 647,1213
Qin, Y.-P. 2008a, ApJ, in press (arXiv:0804.2175)
Qin, Y.-P. 2008b, ApJ, submitted (arXiv:0806.3339)
Rossi, E., Lazzati, D., & Rees, M. J. 2002, MNRAS, 332, 945
Starling, R. L. C. et al. 2008, MNRAS, 384, 504
Tagliaferri, G., Goad, M., Chincarini, G., Moretti, A., et al. 2005, Nature, 436, 985
Wu, X. F. et al. 2006, 36th COSPAR Sci. Ass. #731 (astro-ph/0512555)
Yamazaki et al. 2006, MNRAS, 369, 311
Yonetoku, D. et al. 2008, PASJ, 60, S352
Zhang, B. 2007, ChJAA, 7, 1
Zhang, B., Fan, Y. Z, Dyks, J., Kobayashi, S., et al. 2006, ApJ, 642, 354
Zhang, B. & Mészáros, P. 2002, ApJ, 571, 876
Zhang, B.-B., Liang, E.-W., Zhang, B., 2007, ApJ 666, 1002 (ZLZ07)